Refined Energy Consumption Model of an STA in a Wi-Fi HaLow Network

Sébastien Maudet, Guillaume Andrieux, Romain Chevillon, and Jean-François Diouris

***Abstract*— The deployment of an IoT network is subject to energy consumption constraints. To minimize service costs, it is essential to optimize the lifetime of objects, which are often powered by unreliable energy sources. This optimization must be based on finely-tuned energy consumption models and those generally proposed in the literature do not take into account all the specificities of the transmission of a connected object. In this article, a refined power consumption model based on in-situ measurements is proposed for an 802.11ah station. This improved model takes into account the number of nodes in the network, the number of retransmission attempts and the various exchanges linked to the higher communication layers. The results show the influence of the number of stations in an 802.11ah network on a station's energy consumption, and demonstrate that the maximum number is limited by the probability of successful transmission.**

***Index Terms*— Energy consumption, Internet of Things (IoT), Wi-Fi HaLow, IEEE 802.11ah, wireless sensor network (WSN).**

I. Introduction

ENERGY efficiency is one of the main challenges for IoT networks. In this type of network, the number of devices is large, geographically dispersed and access to energy is unreliable. The Wi-Fi HaLow standard is specifically designed to meet these needs. It operates in sub-GHz frequency bands to improve coverage [1], [2] and natively integrates mechanisms to manage and optimize power consumption for a large number of devices [3], [4]. The long range and large number of supported devices have a direct impact on media availability and, therefore, power consumption. In this way, the Restricted Access Window (RAW) and the Target Wake Time (TWT) can provide fair and collision-free access to the STAtions (STA) [3], [4]. However, the Access Point (AP) needs to know the exact traffic pattern of all STAs to accurately configure these mechanisms. In addition, RAW and TWT are optional, while Distribution Coordination Function (DCF) is the only mandatory feature [1]. All of these factors reinforce the need for accurate modeling of power consumption in 802.11ah IoT networks.

Received 20 August 2024; revised 12 December 2024; accepted 20 January 2025. Date of publication 29 January 2025; date of current version 18 August 2025. This work was supported by La Roche-sur-Yon Agglomération, Région Pays-de-la-Loire and the European Union through the European Regional Development Fund (ERDF) as part of the WISE'Labs Platforms. This work was funded by the French National Research Agency (ANR-22-PEFT-0007) as part of France 2030 and the NF-FITNESS project. The associate editor coordinating the review of this article and approving it for publication was W. Liang. *(Corresponding author: Sébastien Maudet.)*

The authors are with Nantes Université, CNRS, IETR, UMR 6164, 85000 La Roche-sur-Yon, France (e-mail: sebastien.maudet@univ-nantes.fr).

Digital Object Identifier 10.1109/TCOMM.2025.3535868

This article proposes a refined power consumption model for an 802.11ah STA using the DCF mechanism. Based on fine power measurements performed on advanced laboratory equipment, this proposed model is obtained by an absorbing Markov chain, which integrates the specificities of Wi-Fi HaLow and improves the accuracy over previous simulation-based models. Moreover, this refined model takes into account the STA environment by considering both hidden and exposed nodes and the resulting collision probability. This allows scalability to be considered and energy consumption to be studied in detail in dense 802.11ah networks. The results help provide optimization strategies, such as adjusting transmit power and using RTS/CTS to minimize collisions, that can be applied immediately to improve network performance and optimize energy efficiency in IoT deployments.

A. Related Works

Wi-Fi HaLow is a promising IoT technology, and the scientific community has taken a strong interest in it. Its features and open research challenges are reviewed in [3], [4], [5], and [6]. This variant of the Wi-Fi protocol has been the subject of numerous studies, particularly on the physical (PHY) layer [7], propagation models [8], [9], the Media Access Control (MAC) layer [4], and its ability to support various IoT applications [10], [11].

Energy efficiency is an important topic in IoT, and Wi-Fi HaLow is no exception. Some works have developed new mechanisms to improve energy efficiency [12], [13], [14]. However, in order to accurately estimate the lifetime of a node or to correctly size the energy harvester, it is necessary to have a fine energy consumption model that takes into account the 802.11ah specificities. To do this, it is crucial to consider the node in its environment within the IoT network.

While some works provide energy consumption results based on simulations [15], [16], [17], [18], [19], others propose analytical models based on Markov chains, except [20], which presents a closed-form equation model to estimate the average energy consumed by an STA using the RAW mechanism.

The well-known Markov chain model introduced by Bianchi [21] determines the saturated throughput assuming error-free channels and unlimited retransmissions for traditional Wi-Fi technologies. This model has been reinvented several times, for example to consider the effects of short and long retry limits [22] or to study aggregated and block ACK mechanisms [23]. However, these models do not consider the impact of all characteristics on the performance of

media access mechanisms. They typically calculate saturated throughput, delay and packet loss probability, but rarely energy consumption. In addition, Wi-Fi HaLow is designed for IoT with long range and large number of devices, so traditional Wi-Fi models are not directly applicable and energy modeling is critical to evaluate and optimise its performance.

Nevertheless, some studies use Bianchi's closed-loop Markov chain to evaluate the performance of 802.11ah in RAW slots [24], [25] without considering energy consumption. Many other studies investigate energy consumption using analytical models to focus on specific aspects, such as the adaptation of RAW features [26]. Reference [27] developed an analytical model that considers the transmission and collision probabilities of a given STA. Reference [28] extend this model to implement a hybrid contention reservation mechanism for the transmission of uplink traffic.

An original approach is proposed by [29] to investigate the energy problem of an STA operating with RAW or TWT. A Markov process is used to describe the behaviour of a RAW window. The objective is to determine the shortest RAW duration required to transmit all packets from a group of STAs. This model is extended by [30] with the Cross Solt Boundary (CSB) mechanism, by [31] to compute the average energy consumed during a fixed RAW or TWT slot, and by [32] and [33] to assess the probability of timely data delivery for an STA with limited energy harvesting resources.

None of this work on modeling energy consumption takes into account the geographic distribution of nodes. In fact, all nodes use the same Modulation and Coding Scheme (MCS). Furthermore, by assuming that the nodes communicating in the same window are known, hidden STAs are not considered. In addition, all these works focus on the PHY or MAC layers and none of them address the upper layers, such as the network layer. Finally, no analytical model based on real power measurements has been proposed.

B. Contributions and Organization

This paper introduces an analytical model that more accurately describes the energy consumed by an STA in a Wi-Fi HaLow network. Many previous models do not consider the sensor life cycle. Such models are often not based on current measurements, use fixed values to define error probabilities, and fail to integrate the various network layers required for an IoT STA to function correctly. The main contribution of this paper is a refined energy consumption model that takes into account:

- the different communication layers, and therefore the different IP/UDP exchanges, using an absorbing Markov chain,
- the number of STAs present in the network (and their distance from the AP), addressing the issue of hidden and exposed nodes through a geographical distribution of nodes,
- and the different wake-up and transmission phases, using results obtained from measurements of the current and the duration of each phase carried out in our previous work [34].

All these contributions allow us to provide a more comprehensive and realistic framework for energy consumption analysis.

This article is organized as follows. The 802.11ah protocol is briefly introduced in Section II. In-situ measurements that permit the evaluation of the STA energy consumption are presented in Section III and the model is developed in Section IV. The successfull transmission probability and the energy consumed are analysed in Section V for different features and a conclusion is proposed in Section VI.

II. Wi-Fi HaLow Features and Mechanisms

A. Wi-Fi HaLow Overview

Wi-Fi HaLow has been specifically designed to meet the requirements of IoT use cases such as long range, energy efficiency and massive device management. At the PHY layer, the frequency band is sub-GHz and the modulation is Orthogonal Frequency Division Multiplexing (OFDM). PHY features include five BandWidths (BW) (1 to 16 MHz), a dozen MCS (0 to 10), and two Guard Interval (GI) (4 and 8 μs) [3], [5], [6]. BW and GI are in a ratio of 10 compared to 802.11ac, except for the 1 MHz BW that have been added to improve power consumption and increase the transmission range [4], [10], [35]. The energy consumption depends directly on these features, which in turn depend on the link budget, channel conditions and Packet Error Rate (PER).

At MAC layer level, 802.11ah introduces two new media access mechanisms. TWT is recommended when STAs have periodic traffic and need to save energy. RAW is recommended when STAs have on-demand traffic, with a need for fair access and massive downlink. RAW and TWT are optional, DCF/EDCA is the only access mechanism required [1]. In addition, the MAC layer incorporates a new Association IDentification (AID) structure to address up to 8,000 devices, and shortened headers to minimize frame size and thus energy footprint [4], [10], [35].

Wi-Fi HaLow has been calibrated to meet three types of IoT use cases: sensors and meters, backhaul for other IoT data collecting technologies and traditional Wi-Fi network range extension [11]. This article deals with the first use case, whose requirements focus on extending lifetime and reducing sensor operating costs. This use case is generally the one covered by Low Power Wide Area Network (LPWAN) technologies such as LoRa/LoRaWAN, which are characterized by wide coverage and low power consumption [2], [36].

B. Channel Access Mechanisms for Wi-Fi HaLow

1) DCF/EDCA for Unscheduled STA: With DCF, an STA must listen to the media before starting a transmission, in order to minimize collisions and offer fair access to other STAs.

When a frame arrives in the queue, the STA senses the medium. If it's idle for a period equal to the Distributed Inter-Frame Space (DIFS), the STA starts transmission. If it's busy, the STA delays transmission until the medium is again idle for a period equal to DIFS plus a BackOff (BO). The frame is correctly received if the sender receives an ACKnowledgement (ACK). It must wait for an Extended Inter-Frame

TABLE I
EDCA QoS FEATURES FOR A SENSOR STA

AC	SLOT	CW_{min}	CW_{max}	AIFS	SIFS	EIFS
	t_{slot}	W_0	W_m	t_{aifs}	t_{sifs}	t_{eifs}*
BK	52 µs	15	1023	524 µs	160 µs	984 µs
BE	52 µs	3	15	264 µs	160 µs	984 µs
VI	52 µs	7	15	420 µs	160 µs	984 µs
VO	52 µs	7	15	368 µs	160 µs	984 µs

*$t_{eifs} = t_{sifs} + t_{ndp-ack} + t_{aifs}$

Space (EIFS) period before retrying transmission. During the exchange, the sender and receiver keep control of the medium, separating frames by a Short Inter-Frame Space (SIFS).

The BO is an additional random duration. During this period, the STA continues to sense the media while decrementing a BO counter at regular interval t_{slot}. The initial value of the BO counter is an integer randomly selected in $[0, W_n[$. W_n doubles after a failed transmission and it returns to its minimum limit value after a successful transmission. If the medium becomes busy during the BO period, the STA freezes the BO counter and resumes it when the medium becomes idle again. When the BO counter reaches zero, the STA has gained access and can transmit its data frame. The BO period is generated to ensure fair access to the media for other STAs.

EDCA is an extension of DCF that integrates Quality of Service (QoS). The standard defines four service categories for sensor STAs and four others for non-sensor STAs. Table I shows the features of the four sensor Access Categories (AC). The 802.11ah standard specifies that uplink frames from sensor STAs must be mapped to AC_BE [1], [3], [4], [11].

2) Clear Channel Assessment (CCA) and Network Allocation Vector (NAV): An STA must use the "Listen Before Talk" procedure before transmitting a data frame. In the 802.11ah, the CCA-ED can detect interference from other networks if the signal is above −75 dBm for 1 MHz BW and −72 dBm for 2 MHz BW. The CCA-SD can detect transmissions from other STAs in the network if the signal is greater than −98 dBm for a period of 40 µs, or if the signal is greater than −89 dBm for a period of 212 µs [1], [5].

NAV is a virtual carrier sense used at the MAC layer to augment the CCA physical carrier sense. Each frame carries in its MAC header the duration of media occupancy. When another STA is able to read this field, it updates its NAV counter, enabling it to postpone its attempt to access the media after the end of the ACK [3], [4].

The CCA is responsible for detecting the transmission of other STAs. In some cases, other STAs may be out of detection range. To protect against the transmission of hidden nodes, the 802.11ah standard allows STAs to use the Request To Send/Clear To Send (RTS/CTS) mechanism. RTS/CTS frames are transmitted with a more robust modulation scheme [4], [10], [35].

3) Null Data Packet (NDP): The NDP solution promotes fair access and energy efficiency by reducing the size of control and management frames. NDP control frames contains only a PHY header and no MAC header, reducing the size to 6 symbols (i.e. 240 µs) in the case of 2 MHz BW and 14 symbols (i.e. 560 µs) in the case of 1 MHz BW.

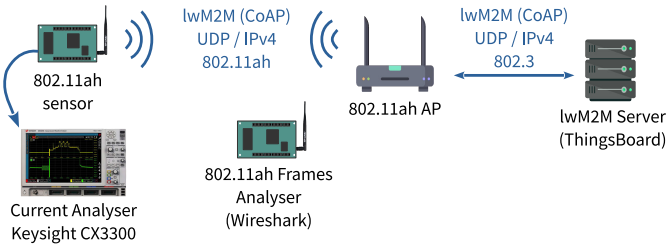

Fig. 1. 802.11ah/lwM2M Testbed implementation.

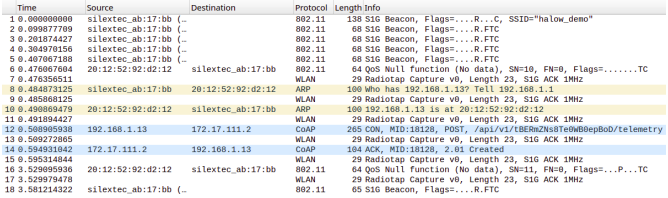

Fig. 2. 802.11ah STA wake-up exchange with the AP.

In 802.11ah, the NDP-CTS and NDP-ACK contain the NAV information in the SIG field of the PHY layer. This Duration is expressed in units of OFDM symbol duration (40 µs).

III. PRACTICAL EVALUATION OF A DATA EXCHANGE

A. Test Bench Implementation

The energy consumption model proposed in this article is based on observation of the operation of an 802.11ah sensor. To this end, a test bench is set up, as shown in Fig. 1 [34].

The 802.11ah sensor is composed of a Silex development board, built around a Newracom NRC-7292 chip and a Qorvo-6901 front-end module [37]. The NRC-7292 contains an 802.11ah Wi-Fi SoC, two Cortex M0 and M3 processors, memory and interfaces essential to the development of an IoT solution [38]. The AP is a Raspberry Pi 3B+ equipped with an Alfa Network APHI-7292 shield [39]. The server is directly connected to the AP and runs an lwM2M solution.

The AP broadcasts a Wi-Fi HaLow SSID at 913.5 MHz with a BW of 1 MHz. An RTS/CTS threshold is configured with variable values in *hostapd.conf* and beacon frames are transmitted every 100 ms. The sensor is placed in deep sleep and wakes up regularly to send JSON-encoded data to the server using the CoAP protocol. UDP, IPv4 and 802.11ah are used in the lower layers and all IP addresses are static.

In addition, another Pi 3B+ equipped with an APHI-7292 shield spies on the Wi-Fi link between the STA and the AP and captures exchanges with wireshark. The current drawn by the STA is measured using a Keysight CX-3300 current analyzer. The current consumed by the STA in each wake-up phases and the duration of each phases are detailed in [34].

B. Exchange Evaluation

Fig. 2 shows a data transmission phase captured by the frame analyzer using wireshark software.

The STA wake-up and starts by sending a QoS *null data* frame to announce its wake-up. This is followed by an ARP frames exchange, that enable the STA to update and verify the network IP/MAC mapping. Then, the frame containing

TABLE II
DURATION OF THE FRAMES EXCHANGED DURING A WAKE-UP

Frame (tr)	MPDU_{tr} (bytes)	$N_{\text{tx},tr}$ / $N_{\text{rx},tr}$*	Variable $t_{tr,mcs}$	Theoretical Values
ARP	66	1/1	$t_{\text{arp},10}$	4200 µs
NDP-ACK	0	2/4	$t_{\text{ack},10}$	560 µs
CoAP (post)	231	1/0	$t_{\text{coap}_{\text{post}},7}$**	1200 µs
CoAP (ack)	70	0/1	$t_{\text{coap}_{\text{ack}},7}$	760 µs
QoS Data	30	2/0	$t_{\text{qos},10}$	2280 µs

* number of frames transmitted and received
** $t_{\text{coap}_{\text{post}},7}$ for 165 bytes transmitted, with MCS7 et 1 MHz BW

the CoAP data is transmitted by the STA to the server. This exchange ends with the transmission of a QoS *null data* frame to announce the STA's return to the deep sleep. All the frames are acknowledged by a NDP-ACK.

C. Length of the Packet and Time on Air

The duration of the frames exchanged between the STA and the AP is given by:

$$t_{tr,mcs} = t_{\text{phy}} + t_{\text{sym}} \cdot \left\lceil \frac{8 \cdot \text{MPDU}_{tr} + N_{\text{serv}} + N_{\text{tail}} \cdot N_{\text{es}}}{N_{\text{dbps}}} \right\rceil, \tag{1}$$

where $t_{tr,mcs}$, t_{phy}, t_{sym}, MPDU_{tr}, N_{serv}, N_{tail}, N_{es} and N_{dbps} are the frame duration ($tr \in [\text{ARP}, \text{RTS}, \text{QoS}, \text{CoAP}]$), the OFDM symbol duration, the PHY header duration, the MAC protocol data unit, the number of bits in the service field, the number of tail bits per Binary Convolutional Coding (BCC) encoder, the number of BCC encoders and the number of data bits per symbol [1], [35].

The frames duration is calculated by using the followig values [1], [35]. $N_{\text{serv}} = 8$ bits, $N_{\text{tail}} = 6$ bits, $N_{\text{es}} = 1$, t_{sym}=40 µs for a long GI and 36 µs for a short GI. t_{phy}=560 µs for 1 MHz BW. N_{dbps} depends on the MCS which in turn depends on the distance from the STA to the AP [1].

Table II synthesis the theoretical duration of the frames. These values are obtained with the equation (1). All these frames are transmitted with the minimum MCS, which is 10 for 1 MHz BW and 0 for 2 MHz BW [1], [35]. CoAP frames are transmitted with the best MCS according to the distance.

All the values collected in our previous work [34] are used to build the energy consumption model described in the following sections.

IV. 802.11ah Station Energy Consumption Model

An 802.11ah STA is in contention when several STAs attempt to access the media. This situation can happen when an STA shares a RAW or TWT access slot with other STAs, or when it operates in *unscheduled* STA mode.

A. 802.11ah Station Environment Model

1) Pathloss Model: The energy consumption model proposed in this section is based on a generic propagation model and a homogeneous distribution of N_{sta} STAs around one AP.

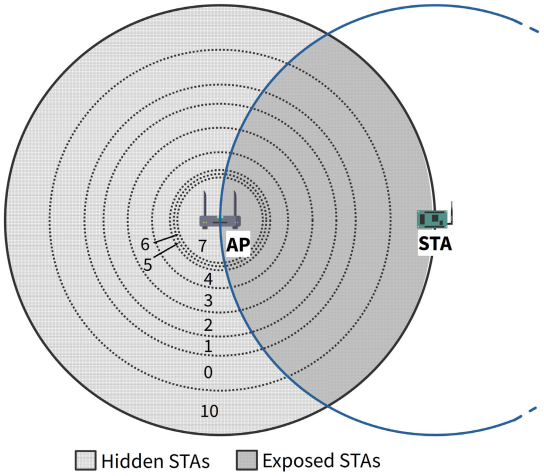

Fig. 3. Hidden and exposed areas for an STA using MCS10.

The STAs µs move and are located at a distance less than or equal to that corresponding to transmission with MCS10. The MCS used to transmit CoAP data depends on this distance and therefore on the propagation model. The distance between the STA and the AP is determined using the isotropic propagation model [8] given by:

$$PL(d_{\text{sta}}) = 20 \cdot \log_{10}\left(\frac{4\pi f_c}{c}\right) + 10 \cdot \gamma \cdot \log_{10}(d_{\text{sta}}), \tag{2}$$

where $PL(d_{\text{sta}})$, d_{sta} and f_c, c and γ are the pathloss model, the distance between the transmitter and the receiver, the carrier frequency, the velocity of the electromagnetic waves and the propagation loss index. For the rest of this article, $\gamma = 3$, $f_c = 913.5$ MHz and $c = 3.10^8$ m/s.

2) Hidden and Exposed STA: Fig. 3 shows an STA at maximum distance from the AP. The AP is surrounded by concentric circles representing the maximum signal reception distance as a function of MCS. STAs using MCS7 are in the first zone around the AP, and so on up to STAs using MCS10. The solid circle around the STA represents its listening area for other transmissions on the network.

The STA's reception and detection capabilities depend on its distance from the AP [40], [41], [42], [43], given by:

$$d_{\text{rx}} = \sqrt[\gamma]{\left(\frac{c}{4\pi f}\right)^2 \cdot \frac{P_{\text{ta}}}{thrd_{\text{rx}}}}, \tag{3}$$

$$d_{\text{csr}} = \sqrt[\gamma]{\left(\frac{c}{4\pi f}\right)^2 \cdot \frac{P_{\text{ta}}}{thrd_{\text{csr}}}}, \tag{4}$$

where d_{rx}, d_{csr}, P_{ta}, $thrd_{\text{rx}}$ and $thrd_{\text{csr}}$ are the reception and the carrier-sense range, the transmission power, and the reception and the carrier-sense threshold, respectively. The reception threshold depends on the MCS used [1], [35] and the carrier-sense threshold is constant and equal to the sensitivity of the MCS10. An STA located within d_{csr} of a transmission in progress must delay its own transmission until the channel is free. All STAs located in the area where the two circles intersect are considered exposed. STAs in the other zone are considered hidden. The area of each zone (hidden and exposed) is determined for each MCS by calculating the area of a "moon". d_{csr} defines the potential

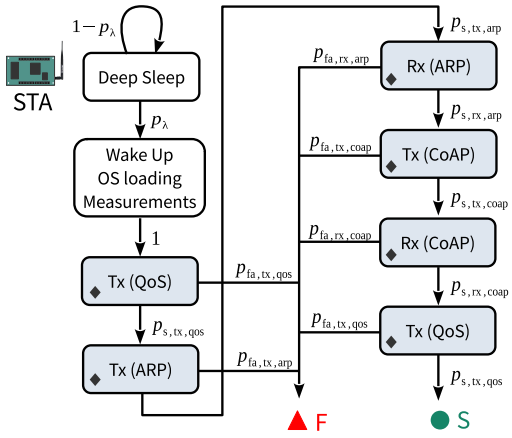

Fig. 4. Absorbing Markov chain modeling of station operations during a wake-up phase.

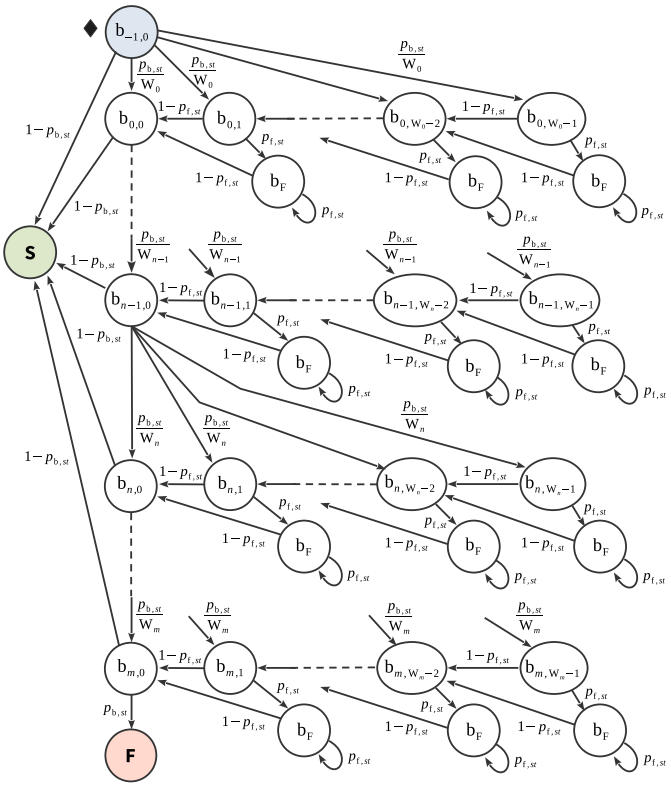

Fig. 5. Absorbing Markov chain modeling of EDCA transmission medium access attempts.

set of exposed nodes [40]. It is assumed that the STAs are uniformly distributed in terms of density around the AP, and have homogeneous physical characteristics in terms of transmission and carrier detection range. The proportion of exposed STA decreases as the distance between STA and AP increases. Conversely, the proportion of hidden STA increases as the distance between STA and AP increases.

The model proposed here is simple and generic. It doesn't take into account the various fading and path loss factors specific to each environment. However, it can easily be replaced by a more complex model.

B. 802.11ah Station Operating Model

1) Wake-up Operation Model: The operation of an 802.11ah STA is modeled using a generic tool based on absorbing Markov chains [43]. It also relies on the Wireshark observation made in section III and the measurements made in [34]. Fig. 4 represents the operations performed by an STA during an operating cycle. The STA doesn't know the state of the other STAs in the network, nor their geographical distribution around the AP. Each STA can wake up and generate data for transmission with probability p_λ.

The STA wakes up, starts its OS, prepares and configures network services, takes physical measurements and transmits data to the server. Transmission operations are marked with a diamond. If all frames are successfully transmitted ($p_{\rm s}$), the Markov chain ends in state ● S. If the transmission of a single frame fails ($p_{\rm fa}$), the Markov chain ends in state ▲ F. Each transmission operation are independently modeled by an absorbing Markov chain, shown in Fig. 5.

2) Transmission Operation Model: This chain defines two absorbing states, labelled S and F. When the STA is in one of the states marked with a diamond on Fig. 4, it transits into the state marked with a diamond on Fig. 5. It then transits through the various states until it reaches one of the absorbing states. Each state corresponds to an operating step of the EDCA mechanism [3], [4], [35].

States $\mathrm{b}_{-1,0}$ to $\mathrm{b}_{m,0}$ represent the $m+2$ transmission attempts allowed. If successful, it enters the absorption state S with probability $1-p_{\mathrm{b},st}$, and leaves the absorption Markov chain. If it fails, it enters one of the states $\mathrm{b}_{n,0}$ to $\mathrm{b}_{n,\mathrm{W}_n-1}$ with probability $\frac{p_{\mathrm{b},st}}{\mathrm{W}_n}$. $p_{\mathrm{b},st}$ represents the probability that another STA starts a transmission or that there is a transmission error.

For each value of $n \in [-1, m]$, the states $\mathrm{b}_{n,0}$ to $\mathrm{b}_{n,\mathrm{W}_n-1}$ represent the slots of the BO period [1], [3], [4], [35]. The maximum value of the BO counter doubles after each failed attempt ($\mathrm{W}_n = 2\cdot \mathrm{W}_{n-1}$). If the STA detects another transmission with probability $p_{\mathrm{f},st}$, it freezes its counter and enters into one of the b_{F} states. When the transmission ends, the STA moves on to the next state with probability of $1-p_{\mathrm{f},st}$.

The EDCA mechanism's contention resolution time is discrete and divided into slots. An STA is only allowed to transmit at the beginning of each slot. A collision is considered when at least two frames are transmitted in the time slot. For competing STAs, the transmission will be successful if no other STA transmits in that slot, and for hidden nodes, the period must be extended to the entire duration of a transmission from the STA under consideration [41], [42], [44]. The values of $p_{\mathrm{b},st}$ and $p_{\mathrm{f},st}$ are given by:

$$p_{\mathrm{b},st} = \begin{cases} 1-(1-\overline{p}_{\mathrm{e},tr,mcs})\cdot(1-\tau)^{N_{\mathrm{e_{sta}}}-1}\cdot(1-\tau)^{s_{\mathrm{vul}}\cdot N_{\mathrm{h_{sta}}}} \\ \qquad\qquad\qquad\qquad\qquad\qquad \text{if } st = \mathrm{tx}, \\ 1-(1-\overline{p}_{\mathrm{e},tr,mcs})\cdot(1-\tau)^{N_{\mathrm{e_{sta}}}+N_{\mathrm{h_{sta}}}} \\ \qquad\qquad\qquad\qquad\qquad\qquad \text{if } st = \mathrm{rx}, \end{cases} \tag{5}$$

$$p_{\mathrm{f},st} = \begin{cases} 1-(1-\tau)^{N_{\mathrm{e_{sta}}}-1}\cdot(1-\tau)^{N_{\mathrm{h_{sta}}}} & \text{if } st = \mathrm{tx}, \\ 1-(1-\tau)^{N_{\mathrm{e_{sta}}}+N_{\mathrm{h_{sta}}}} & \text{if } st = \mathrm{rx}, \end{cases} \tag{6}$$

where τ is the average network load, i.e. the probability of an STA being in a transmission state. $N_{\mathrm{h_{sta}}}$ and $N_{\mathrm{e_{sta}}}$ are the number of hidden and exposed STAs, respectively. $st = \mathrm{tx}$ for an exchange from STA to AP and $st = \mathrm{rx}$ for an exchange from AP to STA.

3) Collision and Transmission Error Probabilities: $p_{\mathrm{b},st}$ is composed of three parts. $(1-\tau)^{N_{\mathrm{e_{sta}}}-1}$ is the probability that no exposed STA transmits data during the transmission attempt and $\left((1-\tau)^{N_{\mathrm{h_{sta}}}}\right)^{s_{\mathrm{vul}}}$ is the probability that no hidden STA transmits data during an extended period of the transmission attempt. s_{vul} corresponds to the vulnerability area of a frame, which is estimated to be equal to 2 times the total duration of a transmission [41], [42], [44]: $s_{\mathrm{vul}} = \left\lceil \frac{2 \cdot \bar{t}_{s,tr}}{\mathrm{t_{slot}}} \right\rceil$. s_{vul} is equal to 0 when the exchange is initiated by the AP to the STA.

$(1-\tau)^{N_{\mathrm{e_{sta}}}-1} \cdot (1-\tau)^{N_{\mathrm{h_{sta}}}}$ represents the probability that no other exposed or hidden STA will transmit data during the BO slot. The values of $N_{\mathrm{e_{sta}}}$ and $N_{\mathrm{h_{sta}}}$ are given by:

$$N_{\mathrm{e_{sta}}} = \sum_{mcs=0}^{10} (p_{\mathrm{e_{sta},}mcs} \cdot N_{\mathrm{sta},mcs}), \tag{7}$$

$$N_{\mathrm{h_{sta}}} = \sum_{mcs=0}^{10} (p_{\mathrm{h_{sta},}mcs} \cdot N_{\mathrm{sta},mcs}), \tag{8}$$

where $N_{\mathrm{sta},mcs}$, $p_{\mathrm{e_{sta},}mcs}$ and $p_{\mathrm{h_{sta},}mcs}$ represent the number of STAs and the percentage of exposed and hidden STAs, respectively. These values are obtained using the generic distribution model proposed in section IV-A.2.

$(1-p_{\mathrm{e},tr,mcs})$ corresponds to the probability of no transmission errors. Reference [45] proposes a mathematical model for calculating the Bit Error Rate (BER) of an OFDM transmission. The PER is given by:

$$p_{\mathrm{e},tr,mcs} = 1 - (1 - \mathrm{BER})^{\frac{1}{\mathrm{R}} \cdot 8 \cdot \mathrm{MPDU}_{tr}}, \tag{9}$$

where $p_{\mathrm{e},tr,mcs}$, R and MPDU_{tr} are the PER of the frame, the modulation code rate and the size of the MPDU, respectively. The values of R and MPDU_{tr} are summarized in [1] and table II.

4) Number of Visits to a Transient State Before Absorption: The absorbing Markov chain shown in Fig. 5 can be written with a four-block transition matrix:

$$\mathrm{M_{r_m \times c_m}} = \begin{bmatrix} \mathrm{Q_{r_q \times c_q}} & \mathrm{R_{r_q \times 2}} \\ 0_{2 \times \mathrm{c_q}} & \mathrm{I_{2 \times 2}} \end{bmatrix}, \tag{10}$$

where $\mathrm{Q_{r_q \times c_q}}$ is the transition between the different states from $\mathrm{b}_{-1,0}$ to $\mathrm{b}_{m,\mathrm{W}_m-1}$. $\mathrm{R_{r_q \times 2}}$ represents the transitions between the transient and the absorbing states. $0_{2 \times \mathrm{c_q}}$ is a null matrix and $\mathrm{I_{2 \times 2}}$ an identity matrix that model the absorbing side of the Markov chain.

When the process begins in a transient state identified as $\mathrm{b}_{n,x}$, the average number of transient state visits before absorption is defined by the fundamental matrix $\mathrm{N_{r_q \times c_q}}$, with $n \in [-1, m]$ and $x \in [\mathrm{W}_n, \mathrm{W}_{n-1}]$. This fundamental matrix is given by:

$$\mathrm{N_{r_q \times c_q}} = \sum_{k=0}^{\infty} \mathrm{Q_{r_q \times c_q}}^{\delta} = (\mathrm{I_{Q_{r_q \times c_q}}} - \mathrm{Q_{r_q \times c_q}})^{-1}, \tag{11}$$

where $\mathrm{I_{Q_{r_q \times c_q}}}$ is an identity matrix and δ represents the number of steps expected to reach the transient state. In this model, the initial state is always $\mathrm{b}_{-1,0}$. It is therefore possible to consider only the first row of the matrix $\mathrm{N_{r_q \times c_q}}$. This vector is denoted $\mathrm{n_{c_q}}$.

C. Success and Failure Probabilities

A packet is successfully transmitted if the matrix $\mathrm{M_{r_m \times c_m}}$ is absorbed by the state S. The same applies to the failure state F. The probability of being absorbed by a given transient state is determined by:

$$\mathrm{B_{r_q \times 2}} = \mathrm{N_{r_q \times c_q}} \cdot \mathrm{R_{r_q \times 2}}. \tag{12}$$

$\mathrm{B_{r_q \times 2}}$ is the absorption matrix. The probabilities of success and failure can therefore be calculated by considering only the vector $\mathrm{n_{c_q}}$, the matrix $\mathrm{R_{r_q \times 2}}$ and the equation (12). The result of this operation is represented by:

$$p_{\mathrm{s},st} = (1 - p_{\mathrm{b},st}) \cdot \sum_{n=0}^{m+1} p_{\mathrm{b},st}^{n}, \tag{13}$$

$$p_{\mathrm{fa},st} = p_{\mathrm{b},st}^{m+2}. \tag{14}$$

D. Average Network Load

A Wi-Fi device operates in half-duplex, which makes collision detection impossible during transmission. When not transmitting, the STA continuously searches for the presence of a physical layer preamble, the unique signature of a Wi-Fi frame. If it detects a preamble, it defers transmission according to the collision avoidance rules of the CSMA/CA mechanism. The collision probability can then be defined as the probability that another STA will start a transmission during a listening time. In this model, the traffic of each network STA is defined as the source of a Poisson process whose intensity and complementary cumulative distribution function are given by:

$$\lambda = \frac{N_{\mathrm{pkt}}}{t_{\mathrm{ts}}}, \tag{15}$$

$$p_{\lambda} = 1 - e^{-\lambda \cdot t_{\mathrm{sleep}}}, \tag{16}$$

where λ, t_{ts} and N_{pkt} are the number of packets generated per second, the time between two wake-ups and the number of packets present in the STA's buffer memory at the wake-up time, respectively. For simplicity, the buffer is considered full when $N_{\mathrm{pkt}} = 1$. The probability of having at least one packet generated by at least one STA in the network during listening times is obtained by estimating the fraction of time an STA spends in one of the transmission states during an operating cycle [46], [47]. This estimation is based on the operation of an STA shown in Fig. 4 and is given by:

$$\tau = \sum_{n=0}^{m+1} \frac{p_{\lambda} \cdot p_{\mathrm{b},st}^{n} \cdot t_{\mathrm{tx}}}{(1-p_{\lambda}) \cdot t_{\mathrm{sleep}} + p_{\lambda} \cdot (t_{\mathrm{wu}} + t_{\mathrm{ech}})}, \tag{17}$$

where t_{tx} and t_{ech} are the time spent by the STA in a transmission state and the average delay of an exchange session, respectively. This delay includes the listening times

of the CSMA/CA mechanism. t_{tx} and t_{ech} are given by:

$$\begin{aligned} t_{\mathrm{tx}} &= N_{\mathrm{tx,qos}}\cdot t_{\mathrm{qos},10} + N_{\mathrm{tx,arp}}\cdot t_{\mathrm{arp},10} + N_{\mathrm{rx,arp}}\cdot t_{\mathrm{arp},10} \\ &\quad + N_{\mathrm{rx,coap}}\cdot \sum_{mcs=0}^{10} (p_{\mathrm{sta},mcs}\cdot t_{\mathrm{coap_{ack}},mcs}) \\ &\quad + N_{\mathrm{tx,coap}}\cdot \sum_{mcs=0}^{10} (p_{\mathrm{sta},mcs}\cdot t_{\mathrm{coap_{post}},mcs}), \end{aligned} \tag{18}$$

$$\begin{aligned} t_{\mathrm{ech}} &= N_{\mathrm{tx,qos}}\cdot D_{\mathrm{qos}} + (N_{\mathrm{tx,arp}} + N_{\mathrm{rx,arp}})\cdot D_{\mathrm{arp}} \\ &\quad + N_{\mathrm{tx,coap}}\cdot D_{\mathrm{coap_{post}}} + N_{\mathrm{rx,coap}}\cdot D_{\mathrm{coap_{ack}}}, \end{aligned} \tag{19}$$

where $N_{\mathrm{tx},tr}$, $N_{\mathrm{rx},tr}$ and D_{tr} are the number of frames exchanged and the average transmission delay of each frame, respectively. D_{tr} is obtained by equation (20), as shown at the bottom of the next page, where $t_{\mathrm{s},tr}$ and $t_{\mathrm{f},tr}$ are the duration of a transmission attempt, resulting in success or failure respectively. The duration of an attempt is given by:

$$t_{\mathrm{s},tr} = \begin{cases} t_{\mathrm{aifs}} + t_{tr,10} + t_{\mathrm{sifs}} + t_{\mathrm{ack}} + 2\cdot t_{\sigma} \\ \qquad \text{if } tr = \mathrm{arp} \text{ or } \mathrm{qos}, \\ t_{\mathrm{aifs}} + \sum_{mcs=0}^{10} (p_{\mathrm{sta},mcs}\cdot t_{tr,mcs}) + t_{\mathrm{sifs}} + t_{\mathrm{ack}} + 2\cdot t_{\sigma} \\ \qquad \text{if } tr = \mathrm{coap_{post}} \text{ or } \mathrm{coap_{ack}}, \end{cases} \tag{21}$$

$$t_{\mathrm{f},tr} = \begin{cases} t_{\mathrm{aifs}} + t_{tr,10} + t_{\sigma} \quad \text{if } tr = \mathrm{arp} \text{ or } \mathrm{qos}, \\ t_{\mathrm{aifs}} + \sum_{mcs=0}^{10} (p_{\mathrm{sta},mcs}\cdot t_{tr,mcs}) + t_{\sigma} \\ \qquad \text{if } tr = \mathrm{coap_{post}} \text{ or } \mathrm{coap_{ack}}. \end{cases} \tag{22}$$

t_{σ} is the waveform propagation time, equal to 6 µs [1], [5], [35]. The equations (5), (6) and (17) represent a non-linear system with three unknowns. The solution is obtained by iteration, knowing that $p_{\mathrm{b},st}, p_{\mathrm{f},st}, \tau \in [0,1]^3$.

E. Expected Energy Consumed by an STA

1) Energy Consumed by an STA for a Transmission: To determine the average energy consumed by an STA during a transmission, it is necessary to estimate the number of visits and the energy consumed by the STA in each state modeled by the absorbing Markov chain. The average energy consumption is obtained by:

$$\overline{\mathrm{e_{r_q}}} = \mathrm{n_{c_q}}\cdot \mathrm{e_{r_q}}, \tag{23}$$

where $\mathrm{e_{r_q}}$ is a vector containing the energy consumed in the various transient states and $\mathrm{n_{c_q}}$ is the vector representing MAC layer protocol operations. The result is given by equation (24), as shown at the bottom of the next page. $\overline{E}_{st,tr}$, $E_{st,-1}$, $E_{st,n}$, $E_{st,-1}$, $E_{st,n}$, $E_{st,\mathrm{slot}}$ and $E_{st,\mathrm{f}}$ represent the average energy consumed by the STA to transmit a frame tr and the energy consumed by the STA in the different states of the Markov chain, respectively.

The energy consumed by the STA in the various states in which a transmission attempt is made ($\mathrm{b}_{n,0}$ with $n \in [-1, m]$) is given by:

$$\begin{aligned} E_{st,-1} = E_{st,n} &= p_{\mathrm{b},st}\cdot (E_{\mathrm{c},st,mcs} + E_{\mathrm{eifs}}) \\ &\quad + (1 - p_{\mathrm{b},st})\cdot E_{\mathrm{s},st,mcs}, \end{aligned} \tag{25}$$

where $E_{\mathrm{s},st,mcs}$ and $E_{\mathrm{c},st,mcs}$ represent the energy consumed in case of success or failure, respectively. E_{eifs} is the energy consumed during the EIFS period. The values of $E_{\mathrm{s},st,mcs}$, $E_{\mathrm{c},st,mcs}$ and E_{eifs} are given by:

$$E_{\mathrm{s},st,mcs} = \begin{cases} \mathrm{V_{sta}}\cdot I_{\mathrm{rx}}\cdot (t_{\mathrm{aifs}} + t_{tr,\mathrm{mcs}} + t_{\mathrm{sifs}} + t_{\sigma}) \\ \quad + \mathrm{V_{sta}}\cdot I_{\mathrm{tx}}\cdot (t_{\mathrm{ack}} + t_{\sigma}) \\ \qquad \text{if } st = \mathrm{rx} \text{ and} \\ \qquad\quad tr \in [\mathrm{coap_{ack}}, \mathrm{arp}], \\ \mathrm{V_{sta}}\cdot I_{\mathrm{rx}}\cdot (t_{\mathrm{aifs}} + t_{\mathrm{sifs}} + t_{\mathrm{ack}} + t_{\sigma}) \\ \quad + \mathrm{V_{sta}}\cdot I_{\mathrm{tx}}\cdot (t_{tr,\mathrm{mcs}} + t_{\sigma}) \\ \qquad \text{if } st = \mathrm{tx} \text{ and} \\ \qquad\quad tr \in [\mathrm{coap_{post}}, \mathrm{qos}, \mathrm{arp}], \end{cases} \tag{26}$$

$$E_{\mathrm{c},st,mcs} = \begin{cases} \mathrm{V_{sta}}\cdot I_{\mathrm{rx}}\cdot (t_{\mathrm{aifs}} + t_{tr,\mathrm{mcs}} + t_{\sigma}) \\ \qquad \text{if } st = \mathrm{rx} \text{ and} \\ \qquad\quad tr \in [\mathrm{coap_{ack}}, \mathrm{arp}], \\ \mathrm{V_{sta}}\cdot [I_{\mathrm{rx}}\cdot t_{\mathrm{aifs}} + I_{\mathrm{tx}}\cdot (t_{tr,\mathrm{mcs}} + t_{\sigma})] \\ \qquad \text{if } st = \mathrm{tx} \text{ and} \\ \qquad\quad tr \in [\mathrm{coap_{post}}, \mathrm{qos}, \mathrm{arp}], \end{cases} \tag{27}$$

$$E_{\mathrm{eifs}} = \mathrm{V_{sta}}\cdot I_{\mathrm{rx}}\cdot t_{\mathrm{eifs}}, \tag{28}$$

where $\mathrm{V_{sta}}$, I_{tx} and I_{rx} are the voltage and currents consumed by the device during transmission and reception, respectively. t_{eifs}, t_{aifs} and t_{sifs} are detailed in table I. I_{tx} and I_{rx} come from the measurements made in [34]. The energy consumed in the states noted from $\mathrm{b}_{0,1}$ to $\mathrm{b}_{m,\mathrm{W}_m-1}$ is given by:

$$E_{\mathrm{slot}} = \mathrm{V_{sta}}\cdot I_{\mathrm{rx}}\cdot t_{\mathrm{slot}}, \tag{29}$$

and the energy consumed in the states noted $\mathrm{b_F}$ is given by:

$$E_{\mathrm{f}} = \sum_{mcs=0}^{10} (p_{\mathrm{e_{sta}},mcs}\cdot E_{\mathrm{e_{tx}},mcs} + p_{\mathrm{h_{sta}},mcs}\cdot E_{\mathrm{h_{tx}},mcs}), \tag{30}$$

where $E_{\mathrm{e_{tx}},mcs}$ and $E_{\mathrm{h_{tx}},mcs}$ represent the energy consumed by the STA when another STA has obtained the media, and the contention counter is frozen. The values of $E_{\mathrm{e_{tx}},mcs}$ and $E_{\mathrm{h_{tx}},mcs}$ are given by:

$$E_{\mathrm{e_{tx}},mcs} = \mathrm{V_{sta}}\cdot I_{\mathrm{rx}}\cdot \overline{t_{\mathrm{s},tr}}, \tag{31}$$

$$E_{\mathrm{h_{tx}},mcs} = \mathrm{V_{sta}}\cdot I_{\mathrm{rx}}\cdot (t_{\mathrm{ack}} + t_{\sigma}). \tag{32}$$

$E_{\mathrm{e_{tx}},mcs}$ is the energy consumed by the STA when the BO counter is frozen for the complete transmission of an exposed STA and $E_{\mathrm{h_{tx}},mcs}$ is the energy consumed by the STA when the BO counter is frozen due to the transmission of an ACK from the AP to a hidden STA.

2) Energy Consumed by an STA for a Complete Wake-up: From the previous equations (24) to (32), it is possible to determine the average energy consumed by an 802.11ah STA during a complete wake-up phase, given by:

$$\begin{aligned}\overline{E}_{\mathrm{tot}} &= E_{\mathrm{wu}} + N_{\mathrm{tx,qos}}\cdot\overline{E}_{\mathrm{tx,qos}} + N_{\mathrm{tx,arp}}\cdot\overline{E}_{\mathrm{tx,arp}} \\ &\quad + N_{\mathrm{rx,arp}}\cdot\overline{E}_{\mathrm{rx,arp}} + N_{\mathrm{tx,coap}}\cdot\overline{E}_{\mathrm{tx,coap}} \\ &\quad + N_{\mathrm{rx,coap}}\cdot\overline{E}_{\mathrm{rx,coap}}, \qquad (33)\end{aligned}$$

$$p_{\mathrm{s}} = \prod_{tr} p_{\mathrm{s,tx}}^{N_{\mathrm{tx},tr}}\cdot\prod_{tr} p_{\mathrm{s,rx}}^{N_{\mathrm{rx},tr}}, \qquad (34)$$

where $\overline{E}_{\mathrm{tot}}$ is the average energy consumed by an STA during a wake-up phase. $\overline{E}_{\mathrm{tot}}$ is equal to the sum of the energies consumed in the different operating states. If the operation represented in Fig. 4 is considered, E_{wu} is obtained from the experiments made in [34]. The values of $N_{\mathrm{tx},tr}$ and $N_{\mathrm{rx},tr}$ are defined in table II and the values of energy consumed in each transmission state are obtained from equations (24) to (32).

V. Energy Consumption Analysis of an 802.11ah Station

A. Numerical Results

In the energy consumption model, equation (2) is used to determine the transmission power and MCS used by the STA, as a function of its distance from the AP. The number of exposed and hidden STAs is then calculated using equations (3) and (4). The error and collision probabilities, as well as the number of packets generated per second are then determined with equations (5), (6), (16) and (17). Finally, equations (24) to (32) and equation (33) can be used to calculate the average energy consumed by an STA during a transmission phase, by varying various input parameters:

- the distance between the 802.11ah STA and the AP,
- the transmission power of the 802.11ah STA,
- the payload carried in CoAP data frame,
- the number of allowed transmission attempts,
- and the duration of the service cycle.

For the results proposed below, we assume that STAs operate with AC_BE QoS category (table I) and they transmit data encapsulated in a CoAP frame with the same duty cycle. The analytical model presented above corresponds to the average energy consumed by an STA. The energy consumed per useful bit is defined by $\overline{E}_{\mathrm{bit}} = \frac{\overline{E}_{\mathrm{tot}}}{8\cdot N_{\mathrm{data}}}$.

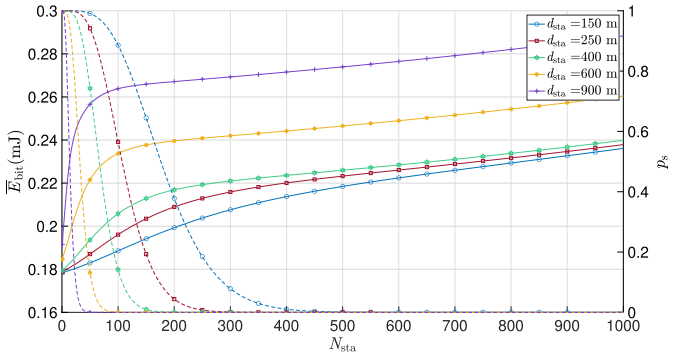

Fig. 6. Probability of successful transmission (dotted line) and average energy consumed per useful bit (solid line) by an 802.11ah STA for different distances vs. the number of STAs in the network (without RTS/CTS, $N_{\mathrm{data}} = 165$ bytes; $P_{\mathrm{ta}} = 23$ dBm; $m = 3$; $t_{\mathrm{ts}} = 30$ s).

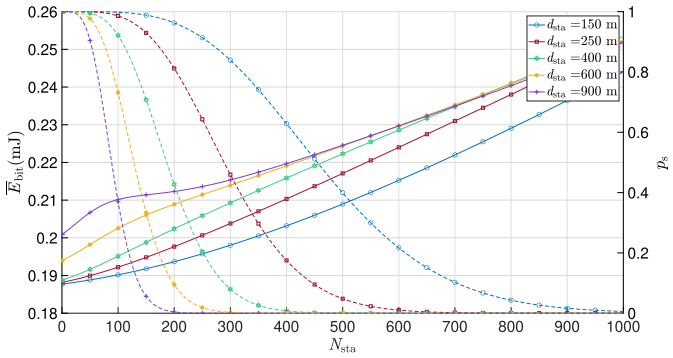

Fig. 7. Probability of successful transmission (dotted line) and average energy consumed per useful bit (solid line) by an 802.11ah STA for different distances vs. the number of STAs in the network (with RTS/CTS, $N_{\mathrm{data}} = 165$ bytes; $P_{\mathrm{ta}} = 23$ dBm; $m = 3$; $t_{\mathrm{ts}} = 30$ s).

Fig. 6 and 7 show the evolution of the successful transmission probability (dotted line) and the average energy consumed per useful bit by an 802.11ah STA (solid line) versus the number of STAs in the network for various distances separating the STA and the AP. The MCS varies with distance, the payload is fixed to 165 bytes, the power at 23 dBm, the number of retries at five and the duty cycle at 30 s. The RTS/CTS is used in Fig. 7 and not in Fig. 6. The value of the successful transmission probability is shown on the right-hand y-axis, and the energy value on the left-hand y-axis.

The average energy consumed per useful bit increases, and the probability of successful transmission decreases with the

$$\begin{aligned}D_{tr} = \sum_{n=0}^{m+1}\left[\left(n\cdot t_{\mathrm{eifs}} + \mathbb{1}_{\{1,m+1\}}(n)\cdot\sum_{k=0}^{n-1}\frac{min(2^k\cdot \mathrm{W}_0, \mathrm{W}_{\mathrm{M}})-1}{2}\cdot t_{\mathrm{slot}} + n\cdot t_{\mathrm{f},tr}\right) + t_{\mathrm{s},tr}\right]\cdot p_{\mathrm{s},st}\cdot p_{\mathrm{b},st}^{n} \\ + \left[(m+1)\cdot t_{\mathrm{eifs}} + \sum_{k=0}^{m}\frac{min(2^k\cdot \mathrm{W}_0, \mathrm{W}_{\mathrm{M}})-1}{2}\cdot t_{\mathrm{slot}} + (m+2)\cdot t_{\mathrm{f},tr}\right]\cdot p_{\mathrm{fa},st}.\end{aligned} \qquad (20)$$

$$\overline{E}_{st,tr} = E_{st,-1} + \sum_{n=0}^{m} p_{\mathrm{b},st}^{n+1}\cdot\left(E_{st,n} + \sum_{k=1}^{2^n \mathrm{W}_0-1}\frac{k}{2^n\cdot \mathrm{W}_0}\cdot\left(E_{\mathrm{slot}} + \frac{p_{\mathrm{f},st}}{1-p_{\mathrm{f},st}}\cdot E_{\mathrm{f}}\right)\right). \qquad (24)$$

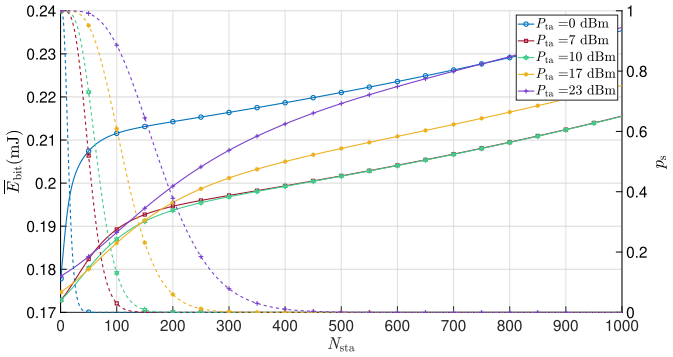

Fig. 8. Probability of successful transmission (dotted line) and average energy consumed per useful bit (solid line) by an 802.11ah STA for different transmission powers vs. the number of STAs in the network (without RTS/CTS, $N_{\text{data}} = 165$ bytes, $m = 3$, $d_{\text{sta}} = 150$ m, $t_{\text{ts}} = 30$ s).

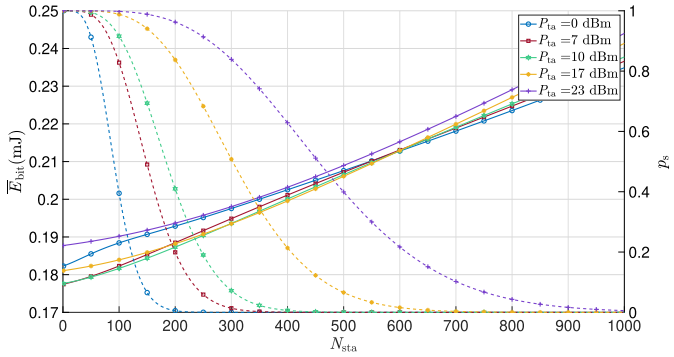

Fig. 9. Probability of successful transmission (dotted line) and average energy consumed per useful bit (solid line) by an 802.11ah STA for different transmission powers vs. the number of STAs in the network (with RTS/CTS, $N_{\text{data}} = 165$ bytes, $m = 3$, $d_{\text{sta}} = 150$ m, $t_{\text{ts}} = 30$ s).

number of STAs in the network. When there is only one STA, the probability of success is close to 100%. The STA then makes a single transmission attempt for each frame, consuming energy of around 0.18 mJ per useful bit transmitted. On the other hand, when there are many STAs, the probability of success is close to 0%, and the STA uses all these attempts to transmit data unsuccessfully. Similarly, as the distance between the STA and the AP increases, the number of hidden STAs increases and the probability of successful transmission decreases, thus increasing energy consumption. In Fig. 6, with 50 STAs in the network, the probability of successful transmission for an STA at 150 m is equal to 99% and 0% for an STA at 900 m. At these distances, the energy consumed per useful bit is equal to 0.182 mJ and 0.256 mJ, respectively. In Fig. 7, with 50 STAs in the network, the probability is greater than 90% whatever the distance. The energy consumed per useful bit is equal to 0.188 mJ for the STA at 150 m and 0.206 mJ for the STA at 900 m. Energy consumption is therefore directly linked to the probability of success, and RTS/CTS greatly reduces collisions, especially for the most distant STAs which are more subject to the hidden nodes problem.

Fig. 8 and 9 show the evolution of the successful transmission probability (dotted line) and the average energy consumed per useful bit by an 802.11ah STA (solid line) versus the number of STAs in the network for various transmit powers. The STA is considered to be 150 m from the AP, the number of attempts is up to five, and the data payload is 165 bytes. STAs generate a packet every 30 s, and transmission power varies from 0 to 23 dBm. The RTS/CTS is used on Fig. 9 and not on Fig. 8. The value of the successful transmission probability is shown on the right-hand y-axis, and the energy value on the left-hand y-axis.

These figures show the same evolution as before. The energy consumed per useful bit and the probability of success evolve with the number of STA in the network. In Fig. 8, for a power of 23 dBm, the probability of success is 99% for 50 STAs, 37% for 200 STAs and 0% for 500 STAs. The average energy consumed per useful bit is then equal to 0.178 mJ, 0.199 mJ and 0.218 mJ, respectively. Beyond 500 STAs, the number of collisions is too high and the device uses the maximum number of retransmissions allowed without successfully transmitting the data. Energy consumption and probability of success also vary with transmission power. The energy consumed per useful bit decreases with the power level, but as the level decreases, so does the MCS. When all the STAs are transmitting at 0 dBm, the one at 150 m uses MCS10, while it uses MCS7 at 23 dBm. At this distance, with 0 dBm, the number of hidden STAs is higher, reducing the probability of success and increasing energy consumption. As a result, the energy consumed by an STA is greater for 0 dBm than 23 dBm. In addition, a single STA in the network consumes the same energy at 0 dBm as at 23 dBm. Indeed, the circuit used in the experiments consumes a current of 112.5 mA at 0 dBm and 357 mA at 23 dBm, but the duration of a frame transmitted with the MCS10 is ten times longer than with the MCS7. In Fig. 9, the RTS/CTS improves the probability of successful transmission, thus reducing energy consumption per useful bit. With 50 nodes in the network, STA consumes 0.185 and 0.188 mJ/useful bit transmitted at 0 and 23 dBm. With 100 nodes in the network, STA consumes 0.193 mJ at both 0 and 23 dBm, but the probability of success is equal to 5% and 96%, respectively. Transmission power is an important parameter, as is the use of RTS/CTS and the number and location of other STAs in the network.

Fig. 10 and 11 show the evolution of the successful transmission probability (dotted line) and the average energy consumed per useful bit by an 802.11ah STA (solid line) versus the number of STAs in the network for various payload carried in the CoAP frame. The transmission power is set to 23 dBm, the number of retransmissions is five, the distance between the STA and the AP is 150 m, the duty cycle is 30 s and the payload varies between 50 and 350 bytes. The RTS/CTS is used in Fig. 11 and not in Fig. 10. The value of the successful transmission probability is shown on the right-hand y-axis, and the energy value on the left-hand y-axis.

The energy consumed per useful bit increases with the number of STAs in the network. It also increases with the payload, in a ratio of one seventh between a load of 50 and 350 bytes. Increasing the payload reduces the amount of energy consumed per useful bit, but increases the transmission time by the same amount, and therefore the area of vulnerability to hidden STA transmissions. In Fig. 10, the probability

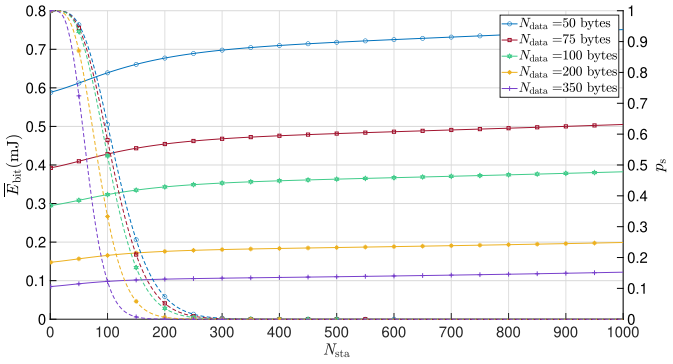

Fig. 10. Probability of successful transmission (dotted line) and average energy consumed per useful bit (solid line) by an 802.11ah STA for different payload values vs. the number of STAs in the network (without RTS/CTS, $m = 3$, $P_{\text{ta}} = 23$ dBm, $d_{\text{sta}} = 150$ m, $t_{\text{ts}} = 30$ s).

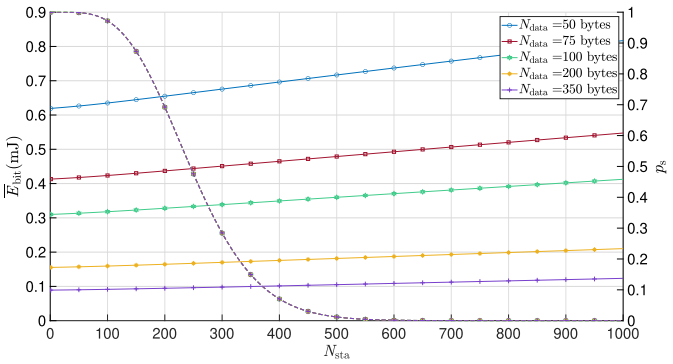

Fig. 11. Probability of successful transmission (dotted line) and average energy consumed per useful bit (solid line) by an 802.11ah STA for different payload values vs. the number of STAs in the network (with RTS/CTS, $m = 3$, $P_{\text{ta}} = 23$ dBm, $d_{\text{sta}} = 150$ m, $t_{\text{ts}} = 30$ s).

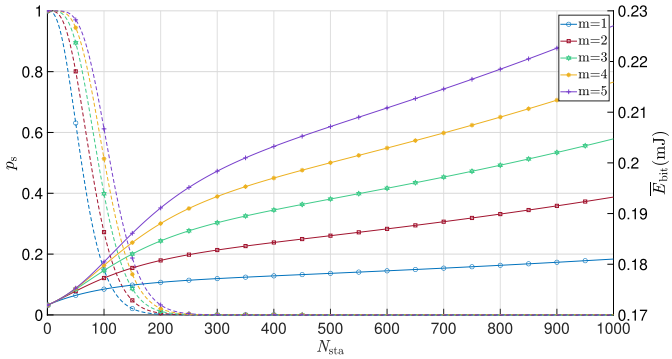

Fig. 12. Probability of successful transmission (dotted line) and average energy consumed per useful bit (solid line) by an 802.11ah STA for different permitted attempts vs. the number of STAs in the network (without RTS/CTS, $N_{\text{data}} = 165$ bytes, $P_{\text{ta}} = 23$ dBm, $d_{\text{sta}} = 150$ m, $t_{\text{ts}} = 30$ s).

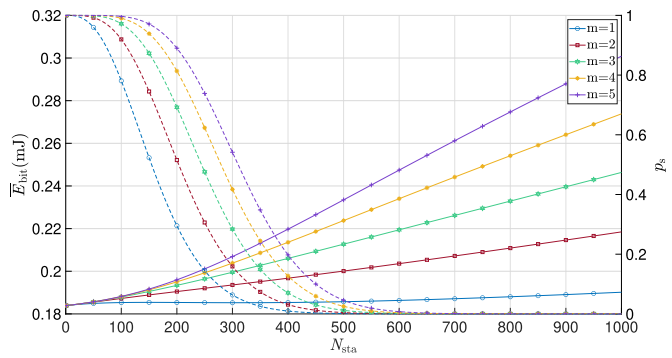

Fig. 13. Probability of successful transmission (dotted line) and average energy consumed per useful bit (solid line) by an 802.11ah STA for different permitted attempts vs. the number of STAs in the network (with RTS/CTS, $N_{\text{data}} = 165$ bytes, $P_{\text{ta}} = 23$ dBm, $d_{\text{sta}} = 150$ m, $t_{\text{ts}} = 30$ s).

of success is close to 0% when the number of STAs exceeds 300 devices. In Fig. 11, the probability of success is close to 0% when the number of STAs exceeds 550 devices. The use of the RTS/CTS has little impact on the energy consumed by an STA close to the AP, but greatly improves the successful transmission probability. The increase in payload associated with the use of the RTS/CTS therefore improves both energy consumption and the successful transmission probability.

Fig. 12 and 13 show the evolution of the successful transmission probability (dotted line) and the average energy consumed per useful bit by an 802.11ah STA (solid line) versus the number of STAs in the network for various number of retries allowed. The payload is set to 165 bytes, the transmit power is 23 dBm, the duty cycle is 30 s and the number of attempts allowed $(m + 2)$ varies between three and seven $(m \in [1, 5])$. The RTS/CTS is used in Fig. 13 and not in Fig. 12. The value of the successful transmission probability is shown on the right-hand y-axis, and the energy value on the left-hand y-axis.

These figures show the same evolution as before. The number of attempts has a low impact on the energy consumed when the successful transmission probability is close to 100%, and a high impact when this probability is close to 0%. In Fig. 12, the successful transmission probability is greater than 90% for three attempts and less than 25 STAs in the network. For seven attempts, it is greater than 90% when there are fewer than 65 STAs. With 25 STAs in the network, the energy consumed is equal to 0.177 mJ/useful bit. With 65 STAs, the energy consumed per useful bit is equal to 0.179 mJ for three attempts and 0.183 mJ for seven attempts. When there are around 200 STAs in the network, the successful transmission probability is less than 3% and the energy consumed per useful bit is equal to 0.183 mJ for three attempts and 0.205 mJ for seven attempts. In Fig. 13, the RTS/CTS improves the successful transmission probability and the energy consumed per useful bit. The number of STAs decreases the probability of success and increases the contention area, which in turn increases energy consumption in proportion to the number of attempts. With the RTS/CTS, the probability is higher. It is equal to 0% beyond 600 STAs. The energy consumed per useful bit is reduced because the STA transmits a less energy-intensive RTS frame before sending its data frame. The risk of collision of an RTS frame with hidden STAs is lower than with a data frame.

Fig. 14 and 15 show the evolution of the successful transmission probability (dotted line) and the average energy consumed per useful bit by an 802.11ah STA (solid line) versus the number of STAs in the network for various duty cycles. The maximum number of attempts allowed is five, the payload is 165 bytes, the distance is 150 m and the power is 23 dBm. The duty cycle varies between 30 and 600 s. The RTS/CTS is used in Fig. 15 and not in Fig. 14. The value of the

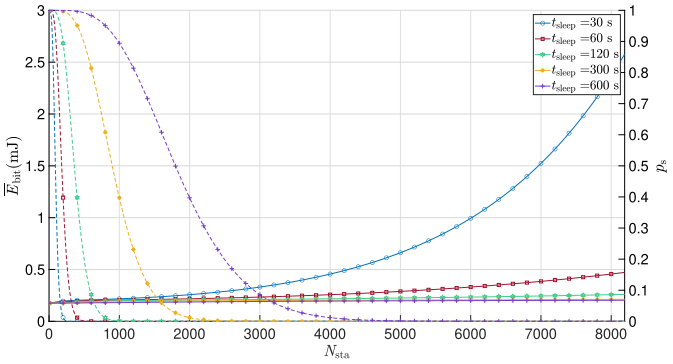

Fig. 14. Probability of successful transmission (dotted line) and average energy consumed per useful bit (solid line) by an 802.11ah STA for different duty cycles vs. the number of STAs in the network (without RTS/CTS, $N_{\text{data}} = 165$ bytes, $P_{\text{ta}} = 23$ dBm, $d_{\text{sta}} = 150$ m, $m = 3$).

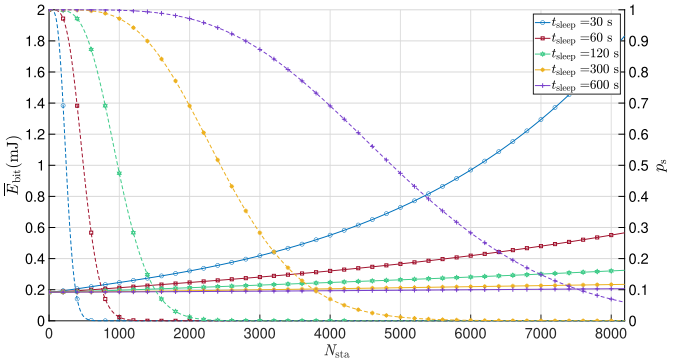

Fig. 15. Probability of successful transmission (dotted line) and average energy consumed per useful bit (solid line) by an 802.11ah STA for different duty cycles vs. the number of STAs in the network (with RTS/CTS, $N_{\text{data}} = 165$ bytes, $P_{\text{ta}} = 23$ dBm, $d_{\text{sta}} = 150$ m, $m = 3$).

successful transmission probability is shown on the right-hand y-axis, and the energy value on the left-hand y-axis. Unlike the previous figures, we have configured the model to obtain the maximum number of STAs supported by an 802.11ah network, which is 8 192.

Once again, the energy consumed by a device increases with the number of STAs in the network. Energy consumption evolves with the probability of success. As the duty cycle increases, the network load (τ) decreases and the probability of successful transmission increases, thus reducing energy consumption. In Fig. 14 with 50 STAs in the network, the energy consumed per useful bit is equal to 0.181 mJ for a 30 s cycle and 0.176 mJ for a 600 s cycle. The successfull transmission probability is equal to 89% and 99%, respectively. When there are 2 000 STAs, the energy consumed per useful bit is equal to 0.257 mJ for a 30 s cycle and 0.185 mJ for a 600 s cycle, but the transmission probabilities are less than 40% for 600 s and 0% for 30 s. In Fig. 15 with 50 STAs in the network, the energy consumed per useful bit is equal to 0.185 mJ for a 30 s cycle and 0.184 mJ for a 600 s cycle. The transmission probabilities are equal to 100%. With 2 000 STAs, the energy consumed per useful bit is equal to 0.320 mJ for a 30 s cycle and 0.188 mJ for a 600 s cycle and the transmission probabilities are equal to 0% and 97%, respectively. The duty cycle has a direct impact on the traffic load and therefore on the number of competing STAs. The results show that it's possible to use DCF with a successful transmission probability of more than 90% for 1000 STAs sending data every 10 min. The RTS/CTS improves this transmission probability and therefore the energy consumption. The maximum number of STAs with a successful transmission probability greater than 90% is reached when the duty cycle is at least 30 min.

B. Discussions

The above results can be put into perspective to open a discussion on optimizing the energy consumption of an 802.11ah STA.

Our model consists of several blocks that can be modified as required. Data traffic is represented by a Poisson process, where arrival times are exponentially distributed. Poisson processes are widely used because they provide a satisfactory description of reality. However, other mathematical tools can be used by modifying the equations (16) and (17). Different traffic can also be modeled for each type of STA by modifying equations (5) and (6). Finally, the STA environment can be modified to better represent the complexity of an IoT network environment, by replacing the propagation model, the density of STAs and the mobility with equations (2), (3), (4), and the vulnerable area of a frame (s_{vul}) in equation (5).

Access to the media is organized on a temporal basis, and the limits are mainly linked to the number of STAs present in the network. To overcome this problem, the standard proposes various solutions: the RTS/CTS collision protection mechanism, which is directly integrated into the DCF/EDCA, the RAW and the TWT energy-saving mechanisms. DCF/EDCA must be implemented in an 802.11ah device, while RAW and TWT are optional [1].

With the DCF/EDCA mechanism, the main problem concerns hidden STAs, which increase the collision probability and the energy consumed in the various attempts. To limit their impact, network STAs must transmit at the maximum power allowed (Fig. 8) in order to make themselves visible to other network STAs. They can also increase the size of the payload (Fig. 10), and so limit the number of wake-ups, which will have the effect of reducing the network load (Fig. 14). Finally, the most remote STAs, which are also those most subject to collisions, can use the RTS/CTS (Fig. 9, 11, 7 and 15) and increase the number of repetitions (Fig. 12 and 13) to maximize their probability of successfully transmitting.

The RAW and TWT mechanisms enable STAs to be grouped according to their needs, and transmission parameters to be fine-tuned. The energy consumed by an STA is equal to 0.17 mJ/useful bit for a load of 165 bytes when it is alone to access the media. This is the case if it is protected by the AP in a RAW or TWT slot. This consumption varies mainly according to load and transmission power.

In addition, the number of STAs in a RAW or TWT group depends mainly on the probability of success. An STA less than 150 m away can compete with 75 STAs with a probability of success greater than 95%. At 900 m, it can compete with fewer than five STAs (Fig. 6). Similarly, a 30 s service cycle will allow 30 STAs to be grouped together, while a 100 s service cycle will enable 90 STAs to be grouped together (Fig. 14). To be optimal, clustering must favor geographic

distribution and minimize hidden STAs. The use of directional antennas at the AP could be a solution to spatially sectorize the environment and minimize hidden STAs.

VI. Conclusion

This paper presents a refined power consumption model for an 802.11ah STA using the DCF mechanism. This analytical model is built from multiple absorbing Markov chains that describe the various exchanges made by an STA using the IP/UDP communication layers. It also takes into account the number of retransmissions and the number of devices in the network, integrating hidden and exposed nodes through a geographic distribution of nodes. To improve the accuracy of the proposed model, in-situ measurements are performed on an 802.11ah testbed, and the results allow us to characterize STA energy consumption and time spent on each 802.11ah communication layer.

In the proposed approach, the frame transmission process is modeled individually by an absorbing Markov chain. This approach allows a more accurate description of a communication protocol and provides the freedom to describe different traffic patterns. This method could be reused to model other communication protocols, such as LoRaWAN or NB-IoT. This would require adapting the absorbing Markov chain to the appropriate media access method and retransmission management method.

The results show the influence of the number of nodes in an 802.11ah network on the energy consumption of an STA. Energy consumption also depends on classical parameters such as transmit power, frame load, number of retransmissions, distance, and duty cycle. In all cases, the energy consumed per useful bit reaches a limit value that depends on the total number of nodes in the network. This demonstrates that the number of STAs that can be integrated into an 802.11ah network is limited due to the collision probability. This paper provides optimization strategies, such as adjusting transmit power and using RTS/CTS to minimize collisions, that can be applied immediately to improve network performance and optimize energy efficiency in IoT deployments.

References

[1] *IEEE Standard for Information Technology—Telecommunications and Information Exchange Between Systems—Local and Metropolitan Area Networks–Specific Requirements—Part 11: Wireless Lan Medium Access Control (MAC) and Physical Layer (PHY) Specifications Amendment 2: Sub 1 GHz License Exempt Operation*, IEEE Standard 802.11ah-2016, 2017, p. 594.

[2] S. Maudet, G. Andrieux, R. Chevillon, and J.-F. Diouris, "Practical evaluation of Wi-Fi HaLow performance," *Internet Things*, vol. 24, Dec. 2023, Art. no. 100957. [Online]. Available: https://www.sciencedirect.com/science/article/pii/S2542660523002809

[3] L. Tian, S. Santi, A. Seferagić, J. Lan, and J. Famaey, "Wi-Fi HaLow for the Internet of Things: An up-to-date survey on IEEE 802.11ah research," *J. Netw. Comput. Appl.*, vol. 182, May 2021, Art. no. 103036. [Online]. Available: https://www.sciencedirect.com/science/article/pii/S108480452100062X

[4] N. Ahmed, D. De, F. A. Barbhuiya, and M. I. Hussain, "MAC protocols for IEEE 802.11ah-based Internet of Things: A survey," *IEEE Internet Things J.*, vol. 9, no. 2, pp. 916–938, Jan. 2022.

[5] L. Qiao, Z. Zheng, W. Cui, and L. Wang, "A survey on Wi-Fi HaLow technology for Internet of Things," in *Proc. 2nd IEEE Conf. Energy Internet Energy Syst. Integr. (EI2)*, Oct. 2018, pp. 1–5.

[6] M. S. Meera and S. N. Rao, "A survey of the state of the art of 802.11ah," in *Proc. IEEE Int. Conf. Comput. Intell. Comput. Res. (ICCIC)*, Dec. 2017, pp. 1–4.

[7] A. Hazmi, J. Rinne, and M. Valkama, "Feasibility study of IEEE 802.11ah radio technology for IoT and M2M use cases," in *Proc. 2012 IEEE Globecom Workshops*, 2012, pp. 1687–1692.

[8] B. Bellekens, L. Tian, P. Boer, M. Weyn, and J. Famaey, "Outdoor IEEE 802.11ah range characterization using validated propagation models," in *Proc. IEEE Global Commun. Conf. (GLOBECOM)*, Dec. 2017, pp. 1–6.

[9] T. De Koninck, S. Santi, J. Famaey, and F. Lemic, "Experimental validation of IEEE 802.11ah propagation models in heterogeneous smarty city environments," in *Proc. IEEE Global Commun. Conf. (GLOBECOM)*, Dec. 2020, pp. 1–6.

[10] Y. Cheng, D. Yang, H. Zhou, and H. Wang, "Adopting IEEE 802.11 MAC for industrial delay-sensitive wireless control and monitoring applications: A survey," *Comput. Netw.*, vol. 157, pp. 41–67, Jul. 2019. [Online]. Available: https://www.sciencedirect.com/science/article/pii/S1389128618308016

[11] S. K. Memon et al., "A survey on 802.11 MAC industrial standards, architecture, security & supporting emergency traffic: Future directions," *J. Ind. Inf. Integr.*, vol. 24, Dec. 2021, Art. no. 100225. [Online]. Available: https://www.sciencedirect.com/science/article/pii/S2452414X2100025X

[12] C. Kai, J. Zhang, X. Zhang, and W. Huang, "Energy-efficient sensor grouping for IEEE 802.11ah networks with max-min fairness guarantees," *IEEE Access*, vol. 7, pp. 102284–102294, 2019.

[13] N. Ahmed and M. I. Hussain, "Periodic traffic scheduling for IEEE 802.11ah networks," *IEEE Commun. Lett.*, vol. 24, no. 7, pp. 1510–1513, Jul. 2020.

[14] Q. T. Ngo, D. N. M. Dang, and Q. Le-Trung, "Extreme power saving directional MAC protocol in IEEE 802.11ah networks," *IET Netw.*, vol. 9, no. 4, pp. 180–188, Jul. 2020. [Online]. Available: https://ietresearch.onlinelibrary.wiley.com/doi/abs/10.1049/iet-net.2019.0176

[15] A. Šljivo et al., "Performance evaluation of IEEE 802.11ah networks with high-throughput bidirectional traffic," *Sensors*, vol. 18, no. 2, p. 325, Jan. 2018. [Online]. Available: https://www.mdpi.com/1424-8220/18/2/325

[16] T.-L. Kao, H.-C. Wang, C.-H. Lu, and T.-H. Cheng, "An energy consumption evaluation of non-TIM strategy in IEEE 802.11ah," *IOP Conf. Ser., Mater. Sci. Eng.*, vol. 644, no. 1, Oct. 2019, Art. no. 012008, doi: 10.1088/1757-899x/644/1/012008.

[17] Z. Zheng, W. Cui, L. Qiao, and J. Guo, "Performance and power consumption analysis of IEEE802.11ah for smart grid," *Wireless Commun. Mobile Comput.*, vol. 2018, no. 1, Jul. 2018, Art. no. 5286560, doi: 10.1155/2018/5286560.

[18] L. Tian, J. Famaey, and S. Latré, "Evaluation of the IEEE 802.11ah restricted access window mechanism for dense IoT networks," in *Proc. IEEE 17th Int. Symp. World Wireless, Mobile Multimedia Netw. (WoWMoM)*, Jun. 2016, pp. 1–9.

[19] L. Tian, M. T. Mehari, S. Santi, S. Latré, E. De Poorter, and J. Famaey, "Multi-objective surrogate modeling for real-time energy-efficient station grouping in IEEE 802.11ah," *Pervas. Mobile Comput.*, vol. 57, pp. 33–48, Jul. 2019. [Online]. Available: https://www.sciencedirect.com/science/article/pii/S1574119218305819

[20] A. Bel, T. Adame, and B. Bellalta, "An energy consumption model for IEEE 802.11ah WLANs," *Ad Hoc Netw.*, vol. 72, pp. 14–26, Apr. 2018. [Online]. Available: https://www.sciencedirect.com/science/article/pii/S1570870518300052

[21] G. Bianchi, "Performance analysis of the IEEE 802.11 distributed coordination function," *IEEE J. Sel. Areas Commun.*, vol. 18, no. 3, pp. 535–547, Mar. 2000.

[22] H. Wu, Y. Peng, K. Long, S. Cheng, and J. Ma, "Performance of reliable transport protocol over IEEE 802.11 wireless LAN: Analysis and enhancement," in *Proc. 21st Annu. Joint Conf. IEEE Comput. Commun. Societies*, vol. 2, Mar. 2002, pp. 599–607.

[23] M. A. Hossain, N. I. Sarkar, J. Gutierrez, and W. Liu, "Performance study of block ACK and reverse direction in IEEE 802.11n using a Markov chain model," *J. Netw. Comput. Appl.*, vol. 78, pp. 170–179, Jan. 2017. [Online]. Available: https://www.sciencedirect.com/science/article/pii/S108480451630296X

[24] U. Sangeetha and A. V. Babu, "Service differentiation in IEEE 802.11ah WLAN under restricted access window based MAC protocol," *Comput. Commun.*, vol. 172, pp. 142–154, Apr. 2021. [Online]. Available: https://www.sciencedirect.com/science/article/pii/S0140366421001195

[25] S. M. Soares and M. M. Carvalho, "An analytical model for the aggregate throughput of IEEE 802.11ah networks under the restricted access window mechanism," *Sensors*, vol. 22, no. 15, p. 5561, Jul. 2022. [Online]. Available: https://www.mdpi.com/1424-8220/22/15/5561

[26] Y. Wang, Y. Li, K. K. Chai, Y. Chen, and J. Schormans, "Energy-aware adaptive restricted access window for IEEE 802.11ah based networks," in *Proc. IEEE 26th Annu. Int. Symp. Pers., Indoor, Mobile Radio Commun. (PIMRC)*, Aug. 2015, pp. 1211–1215.

[27] R. P. Liu, G. J. Sutton, and I. B. Collings, "Power save with offset listen interval for IEEE 802.11ah smart grid communications," in *Proc. IEEE Int. Conf. Commun. (ICC)*, Jun. 2013, pp. 4488–4492.

[28] L. Beltramelli, P. Österberg, U. Jennehag, and M. Gidlund, "Hybrid MAC mechanism for energy efficient communication in IEEE 802.11ah," in *Proc. IEEE Int. Conf. Ind. Technol. (ICIT)*, Mar. 2017, pp. 1295–1300.

[29] E. Khorov, A. Krotov, and A. Lyakhov, "Modelling machine type communication in IEEE 802.11ah networks," in *Proc. IEEE Int. Conf. Commun. Workshop (ICCW)*, Jun. 2015, pp. 1149–1154.

[30] E. Khorov, A. Lyakhov, and R. Yusupov, "Two-slot based model of the IEEE 802.11ah restricted access window with enabled transmissions crossing slot boundaries," in *Proc. IEEE 19th Int. Symp. World Wireless, Mobile Multimedia Netw. (WoWMoM)*, Jun. 2018, pp. 1–9.

[31] S. Santi, L. Tian, E. Khorov, and J. Famaey, "Accurate energy modeling and characterization of IEEE 802.11ah RAW and TWT," *Sensors*, vol. 19, no. 11, p. 2614, Jun. 2019. [Online]. Available: https://www.mdpi.com/1424-8220/19/11/2614

[32] D. Bankov, E. Khorov, A. Lyakhov, and J. Famaey, "Resource allocation for machine-type communication of energy-harvesting devices in Wi-Fi HaLow networks," *Sensors*, vol. 20, no. 9, p. 2449, Apr. 2020. [Online]. Available: https://www.mdpi.com/1424-8220/20/9/2449

[33] E. Zazhigina, R. Yusupov, A. Lyakhov, and E. Khorov, "Analytical study of restricted access window with short slots for fast and reliable data delivery from energy-harvesting sensors," *Comput. Netw.*, vol. 250, Aug. 2024, Art. no. 110573. [Online]. Available: https://www.sciencedirect.com/science/article/pii/S1389128624004055

[34] S. Maudet, G. Andrieux, R. Chevillon, and J.-F. Diouris, "Evaluation and analysis of the Wi-Fi HaLow energy consumption," *IEEE Internet Things J.*, vol. 11, no. 17, pp. 28244–28252, Sep. 2024.

[35] V. Baños-Gonzalez, M. Afaqui, E. Lopez-Aguilera, and E. Garcia-Villegas, "IEEE 802.11ah: A technology to face the IoT challenge," *Sensors*, vol. 16, no. 11, p. 1960, Nov. 2016. [Online]. Available: https://www.mdpi.com/1424-8220/16/11/1960

[36] Wireless Broadband Alliance, Morse Micro, Newracom, Methods2Business. (2024). *Wi-Fi HaLow for IoT Field Trials Report*. [Online]. Available: https://wballiance.com/resource/wi-fi-halow-for-iot-field-trials-report/

[37] Silex_Technology. (2023). *SX-NEWAH Evaluation Kit*. [Online]. Available: https://www.silextechnology.com/connectivity-solutions/embedded-wireless/sx-newah-evaluation

[38] Newracom. (2023). *NRC7292*. [Online]. Available: https://newracom.com/products/nrc7292

[39] Alfa_Network. (2023). *AHPI7292S*. [Online]. Available: https://www.alfa.com.tw/products/ahpi7292s

[40] Y. Zhou and S. M. Nettles, "Balancing the hidden and exposed node problems with power control in CSMA/CA-based wireless networks," in *Proc. IEEE Wireless Commun. Netw. Conf.*, vol. 2, May 2005, pp. 683–688.

[41] S.-G. Yoon, J.-O. Seo, and S. Bahk, "Regrouping algorithm to alleviate the hidden node problem in 802.11ah networks," *Comput. Netw.*, vol. 105, pp. 22–32, Aug. 2016. [Online]. Available: https://www.sciencedirect.com/science/article/pii/S1389128616301487

[42] S. Kumar, S. Choi, and H. Kim, "Analysis of hidden terminal's effect on the performance of vehicular ad-hoc networks," *EURASIP J. Wireless Commun. Netw.*, vol. 2019, no. 1, p. 240, Oct. 2019, doi: 10.1186/s13638-019-1548-4.

[43] F. A. Aoudia, M. Gautier, M. Magno, O. Berder, and L. Benini, "A generic framework for modeling MAC protocols in wireless sensor networks," *IEEE/ACM Trans. Netw.*, vol. 25, no. 3, pp. 1489–1500, Jun. 2017.

[44] O. Ekici and A. Yongacoglu, "IEEE 802.11a throughput performance with hidden nodes," *IEEE Commun. Lett.*, vol. 12, no. 6, pp. 465–467, Jun. 2008.

[45] J. van Wyk and L. Linde, "Bit error probability for a M-ary QAM OFDM-based system," in *Proc. AFRICON*, Sep. 2007, pp. 1–5.

[46] A. Tsarev, E. Khayrov, E. Medvedeva, Y. Gaidamaka, and C. Buratti, "Analytical model for CSMA-based MAC protocol for industrial IoT applications," in *Internet of Things, Smart Spaces, and Next Generation Networks and Systems*, O. Galinina, S. Andreev, S. Balandin, and Y. Koucheryavy, Eds., Cham, Switzerland: Springer, 2020, pp. 240–258.

[47] K. E. Samouylov, Y. V. Gaidamaka, I. A. Gudkova, E. R. Zaripova, and S. Y. Shorgin, "Baseline analytical model for machine-type communications over 3GPP RACH in LTE-advanced networks," in *Computer and Information Sciences*, T. Czachórski, E. Gelenbe, K. Grochla, and R. Lent, Eds., Cham, Switzerland: Springer, 2016, pp. 203–213.